Available online at www.sciencedirect.com
ScienceDirect
Ceramics International 35 (2009) 2409–2414
CERAMICS INTERNATIONAL
www.elsevier.com/locate/ceramint

Tip deflection calculations of small-diameter thin-walled piezoelectric tubes

M. Leung [a], E. Haemmerle [a,*], M. Hodgson [b], W. Chen [b], W. Gao [b]

[a] Department of Mechanical Engineering, The University of Auckland, Private Bag 92019, Auckland 1010, New Zealand
[b] Department of Chemical and Materials Engineering, The University of Auckland, Private Bag 92019, Auckland 1010, New Zealand

Received 9 September 2008; received in revised form 13 September 2008; accepted 2 February 2009
Available online 25 February 2009

Abstract

Piezoelectric tubes with various dimensions were fabricated using the electrophoretic deposition (EPD) process. The tubes are aimed to be used as actuators in fiber-optic switches which require a tip deflection of at least 65 μm. To maximize the tip deflection of the tubes and to achieve multiple-direction switching, the tubes had an unique electrode arrangement and, therefore, new analytic equations were needed to analyze their tip deflection. Equations for thick-walled and thin-walled piezoelectric tubes were developed by modifying existing equations which could be used to estimate the performance of new tubes and to optimize their dimensions for different applications. Experimental verification showed that the new equations gave a good estimation of the new piezoelectric tubes' deflection. The advantages and limitations of the modified equations are also discussed.

Keywords: C. Piezoelectric properties; C. Mechanical properties; D. PZT; E. Actuator

1. Introduction

Piezoelectric actuators, such as tubes and bimorphs, can magnify a small strain into a large displacement. A tube can easily deflect in all directions and is simpler in construction than a flat-type actuator such as a bimorph. Chen [1] and Li [2] have derived equations to estimate the tip deflection of tubes. To simplify mathematics, Chen assumed that the wall thickness of the tubes was much smaller than the diameter, and that two of the four outer electrodes were grounded as shown in Fig. 1(a). Chen measured the tip deflection of tubes of 6.35 mm radius, wall thickness of 1.02 mm and various lengths and found that the results agreed well with the theoretical estimates. Li manufactured small double-layered tubes with an inner and outer radius of 1.6 mm and 1.8 mm, respectively, whereby the inner and outer layers were separated by an embedded intermediate electrode with a radius of 1.71 mm. The drive voltage was applied as shown in Fig. 1(b), allowing deflection in two directions. The calculated (theoretical) and measured tube tip deflection results were compared and found to be in good agreement.

Both Li's and Chen's tip deflection equations were developed for thin-walled tubes, without explicitly stating what constituted a thin- or thick-walled tube. Many commercially available tubes are of larger wall thickness than Li and Chen have used. It is not known whether their equations are applicable for these tubes. Li has compared calculated and measured tip deflections of small-diameter tubes, whereas Chen has done the same for larger diameter tubes. To the best of the authors' knowledge, no comparison between the two tip deflection equations has been published so far. Applications which require large deflections are better served by small-diameter tubes. The fiber-optic switch [3,4] application of piezoelectric tubes described here requires a four-sectored electrode configuration allowing bending in four directions as shown in Fig. 1(c). Hence, there is a need to investigate the accuracy and appropriateness of the two equations. Their merits and limitations will be described in light of the given application requirements.

* Corresponding author. Tel.: +64 9 373 7599.
E-mail address: e.haemmerle@auckland.ac.nz (E. Haemmerle).

0272-8842/$34.00
doi:10.1016/j.ceramint.2009.02.004

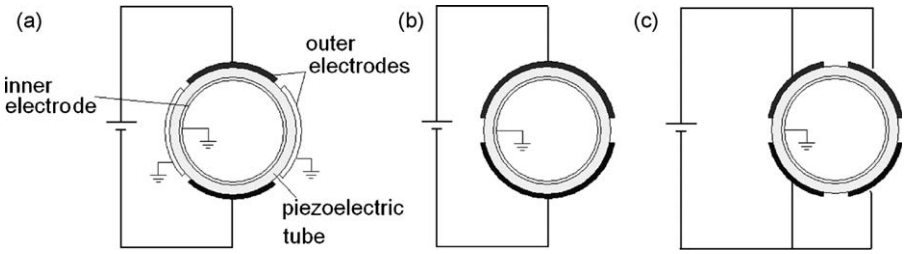

Fig. 1. Electrode configurations: (a) Chen; (b) Li; (c) fiber-optic switch application.

2. Electrophoretic deposition process (EPD)

Several piezoelectric tubes (Fig. 2) of different wall thicknesses, diameters and lengths as listed in Table 1 have been fabricated using the electrophoretic deposition (EPD) process [5].

EPD started with piezoceramic powder being suspended in an ethanol solution in a stainless steel container. The powder used was a combination of lead zirconate titanate (PZT) and lead magnesium niobium oxide (PZT–PMN), near the morphotropic phase boundary with a composition of $0.9Pb(Zr_{0.52}Ti_{0.48})O_3–0.1Pb(Mg_{1/3}Nb_{2/3})O_3$. This soft piezoceramic composition is known to have excellent dielectric and piezoelectric properties. The PZT–PMN system synergistically combined the properties of both normal ferroelectric PZT and relaxor ferroelectric PMN, exhibiting better dielectric and piezoelectric properties than the single-phase PZT and PMN. The pH value of the PZT–PMN powder-ethanol suspension was adjusted to 4.5 with the addition of nitric acid. The suspension was stirred for 3–6 h to ensure complete dispersion of the powder. The electrophoretic cell included a cathodic carbon rod of specific diameter placed in the center of the anodic stainless steel container. Deposition was performed by applying 100 V to the electrophoretic cell for 2–5 min, depending on the desired thickness of the tube. After the EPD process, the tubes were sintered at 1250 °C for 2 h and subsequently coated with silver conductive paint on the inner and outer surfaces before they were poled. Fig. 3 shows the cross-section of one of the tube samples indicating that the silver electrode coating on the tube is uniform with a thickness of around 0.01 mm.

After the poling process, the outer electrode coating could be sectored resulting in either two (as shown in Fig. 4) or four electrodes.

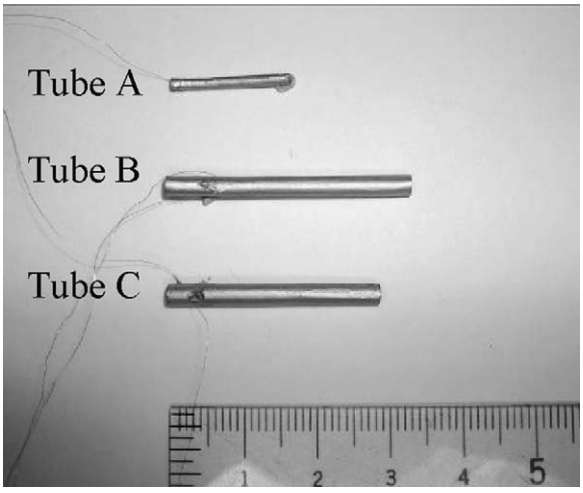

Fig. 2. Sample tubes.

Table 1
Dimensions of the piezoelectric tube samples.

	Tube A	Tube B	Tube C
Inner radius (mm)	0.49	1.09	1.17
Outer radius (mm)	0.80	1.41	1.44
Length (mm)	16.0	33.9	28.0
Wall to inner radius ratio	0.63	0.30	0.23
Electrode gap width (mm)	0.4	0.35	0.35

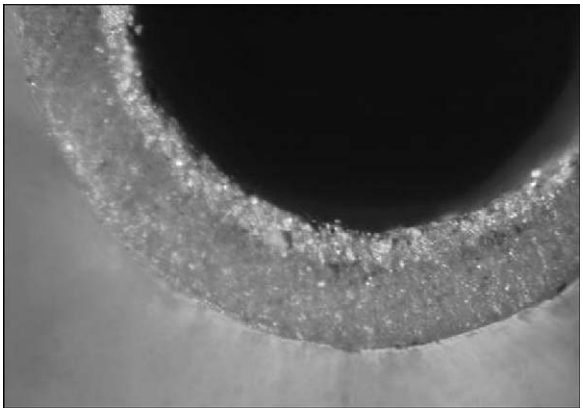

Fig. 3. Cross-section of a piezoelectric tube.

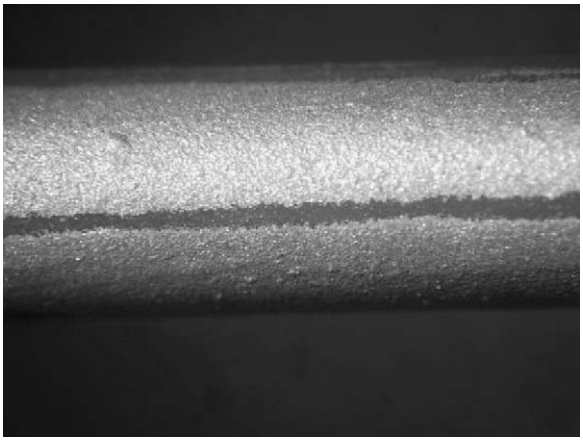

Fig. 4. Electrode gap of a piezoelectric tube sample.

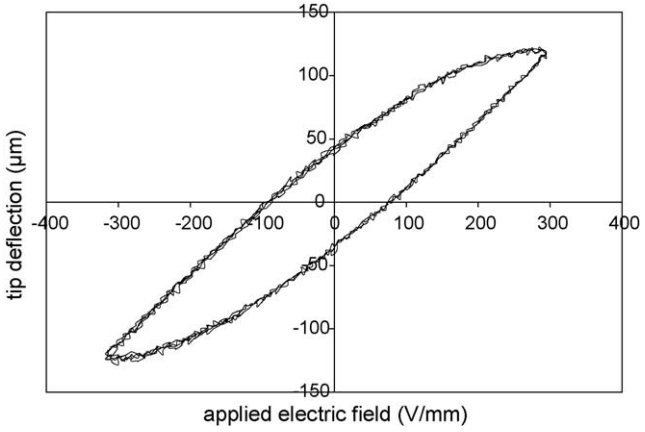

Fig. 5. Tip deflection hysteresis loop of a piezoelectric tube sample.

The piezoelectric tubes fabricated have been designed to achieve maximum deflection so that they can be used as fiber-optic switch actuators. Fig. 5 demonstrates the achievable tip deflection capability.

3. Original tip deflection equations

The tip deflections of the fabricated tubes, as listed in Table 1, have been measured and compared to the theoretical estimates by Lin and Chen. Fig. 6 shows the results for Tube A with two and four sectored electrodes. The electrode gaps were 0.5 mm wide.

The single-layer version of the equation derived by Li, $\xi_{Li.} = (-4d_{31}V\cos\beta L^2)/(\pi(r_o^2 + r_i^2)\ln(r_o/r_i))$, showed good agreement for the two-electrode version, but was less appropriate for the four-electrode version. Specifically, for small-diameter tubes with wider electrode gaps, Li's equation did not account for the two electrode gaps. The equation by Chen, $\xi_{Chen} = \sqrt{2}d_{31}VL^2/\pi rt$, was developed for thin-walled tubes and hence showed to be inappropriate for the given thick-walled Tube A. For these reasons, the limitations of the above-mentioned tip deflection equations have been further analyzed and their applicability to model tubes of various wall thicknesses, number of electrodes, gap widths between electrodes and tube diameters were investigated.

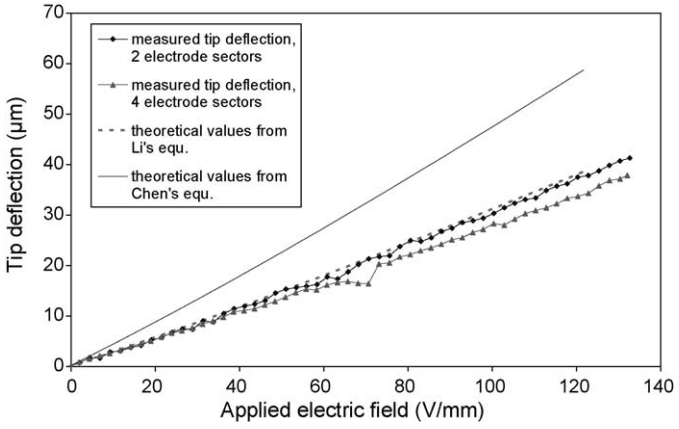

Fig. 6. Tip deflection of Tube A.

4. Modified tip deflection equations

Fig. 7 depicts the cross-section of a multi-sectored piezoelectric tube. The tube allowed deflection in four different directions and was suitable to be used as a switching element in 1×4 fiber-optic switch. Due to the symmetry of the tube, only a quarter of the tube's cross-section was considered. When voltage was applied to the tube, the portion of the tube covered by electrodes experienced strain and generated a bending moment. At the sector when $\alpha \le \theta \le \beta$, the stress along the tube T_1 is

$$T_1 = \frac{S_1}{s_{11}^E} - \frac{E_3 d_{31}}{s_{11}^E}, \tag{1}$$

where S_1 is the strain along the tube, d_{31} is the piezoelectric charge constant, s_{11}^E is the compliance constant under constant electric field, and E_3 is the electric field across the wall. For a cylindrical sample, the electric field at a particular radius r is

$$E_3 = \frac{V}{r\ln(r_o/r_i)}, \tag{2}$$

where V is the applied voltage, and r_o and r_i are the outer and inner radii of the tube, respectively. At the sector of the tube when $0 \le \theta < \alpha$ and $\beta < \theta \le \pi/2$, the tube is not covered by electrodes so that $E_3 = 0$. The stress along the Z-direction is

$$T_1 = \frac{S_1}{s_{11}^E}. \tag{3}$$

The total bending moment along the cross-section of the tube is zero at equilibrium. Therefore,

$$\int_{area} T_1(r\sin\theta)\,dA = 0 \tag{4}$$

$$\int_{r_i}^{r_o}\int_0^{\alpha} \frac{-(r\sin\theta)^2}{s_{11}^E\rho_r} r\,d\theta\,dr + \int_{r_i}^{r_o}\int_{\alpha}^{\beta}\left(\frac{-(r\sin\theta)^2}{s_{11}^E\rho_r} - \frac{Vd_{31}\sin\theta}{\ln\left(\frac{r_o}{r_i}\right)s_{11}^E}\right) r\,d\theta\,dr + \int_{r_i}^{r_o}\int_{\beta}^{\pi/2} \frac{-(r\sin\theta)^2}{2s_{11}^E\rho_r} r\,d\theta\,dr = 0 \tag{5}$$

$$\frac{1}{\rho_r} = \frac{8Vd_{31}(r_o^2 - r_i^2)(\cos\alpha - \cos\beta)}{\pi\ln(r_o/r_i)(r_i^4 - r_o^4)}. \tag{6}$$

Based on Eq. (6) and the tip deflection formula for a cantilevered beam experiencing a bending moment, $\xi = L^2/2\rho_r$ [6], the modified tip deflection $\xi_{Li.Mod.}$ based on Li's equation is modified into

$$\xi_{Li.Mod.} = \frac{-4d_{31}VL^2(\cos\alpha - \cos\beta)}{\pi(r_o^2 + r_i^2)\ln(r_o/r_i)} \tag{7}$$

The difference between Li's original and the modified equation is the extra term $-\cos\beta$ which accounts for the additional

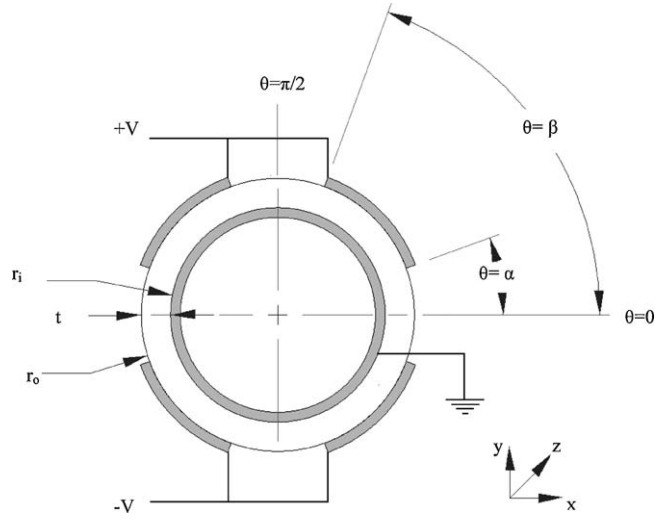

Fig. 7. Electrode configuration of a multi-sectored piezoelectric tube.

electrode gaps as illustrated in Fig. 7. For tubes with large outer diameters and small electrode gaps, the additional $-\cos\beta$ term is not significant. However, when modeling small-diameter tubes with wider electrode gaps, the modified equation more closely predicts the tip deflection than the original one.

Based on a similar methodology, the equation developed by Chen, $\xi_{Chen} = \sqrt{2}d_{31}VL^2/\pi rt$, is modified to

$$\xi_{Chen.Mod.} = \frac{2d_{31}VL^2(\cos\alpha - \cos\beta)}{\pi rt} \tag{8}$$

The modified Chen equation has a different coefficient and an additional term $(\cos\alpha - \cos\beta)$ which models the four-electrode gaps of various gap widths.

5. Comparison between the two modified equations for thin- and thick-walled piezoelectric tubes

This section will quantify the differences and accuracies of the two modified equations and to assess their suitability for different tube sizes and electrode configurations, as indicated in Table 1 and Fig. 2.

To calculate the tip deflection of the piezoelectric tube samples, it is necessary to know the piezoelectric charge constant of the material. The piezoelectric tubes will be used as actuators where a strong electric field is applied to the tube to produce large tip deflections. Under a strong electric field, the piezoelectric material experiences non-180° domain-wall motions. The strain and applied field relationship is non-linear and significant hysteresis occurs [7]. In this case, the strain of a stress-free piezoelectric tube can be expressed as

$$S_3 = d_{31}(E)E_1, \tag{9}$$

where the piezoelectric charge constant, $d_{31}(E)$, is a function of the electric field. $d_{31}(E)$ was obtained by measuring the strain at different applied fields of the piezoelectric tube samples. Fig. 8 depicts the strain versus electric field relationship of Tube A. The tube was coated on both inner and outer surfaces with the outer surface not yet sectored. Voltages from 0 V to ±120 V were applied to the inner and outer surfaces and the strains of the tube were measured using a Hamamatsu S2044 Position Sensitive Detector. The measured $d_{31}(E)$ can be used to estimate the tip deflection of the tube samples.

Fig. 9 shows the theoretical tip deflection estimates using the modified equations. The calculations are based on an inner tube diameter of 1 mm and a drive voltage of 100 V. The graph illustrates that with a 'wall thickness to radius' ratio of 0.25 or less, the difference between the results from the two equations is less than 15%. For a tube with a 'wall thickness to radius' ratio greater than 0.25, the difference in estimated tip deflection from the two equations becomes more significant.

To verify the accuracy of the modified formulae, the tip deflections of a number of piezoelectric tubes were measured and the results were compared with the theoretical values calculated using the modified equations. Fig. 10 displays the theoretical estimates and the measured tip deflections of Tube A at varying electric fields. Tube A has a comparatively thick wall with a 'wall thickness to radius' ratio of 0.63. The results show that the measured deflections of Tube A match well with the calculated values from the modified Li equation. The estimated tip deflections from the modified Chen equation and the measured values, however, deviate significantly. Chen's modified equation on average over-estimates by 31% when

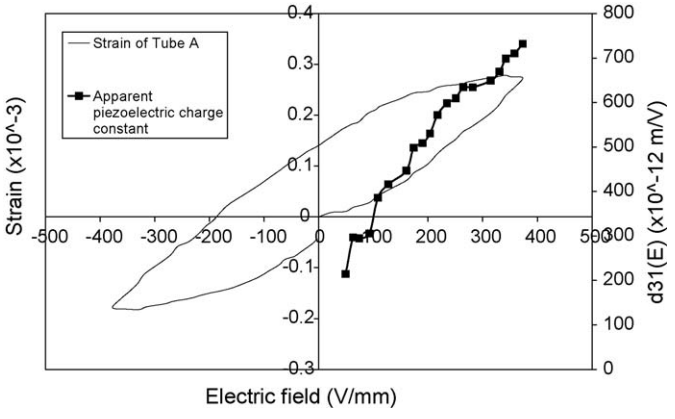

Fig. 8. Strain along Z-direction of Tube A.

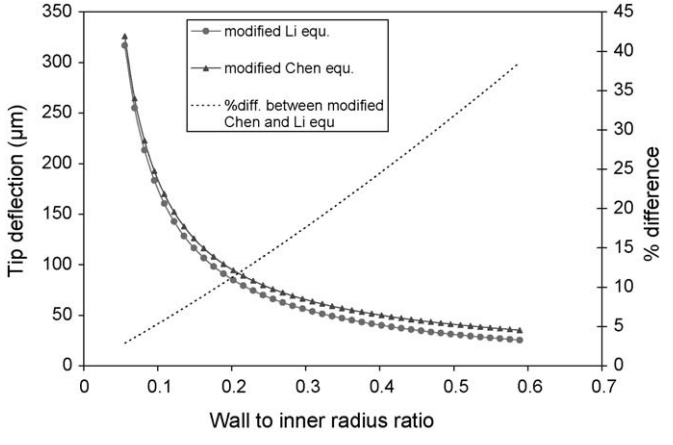

Fig. 9. Theoretical tip deflection values of piezoelectric tubes.

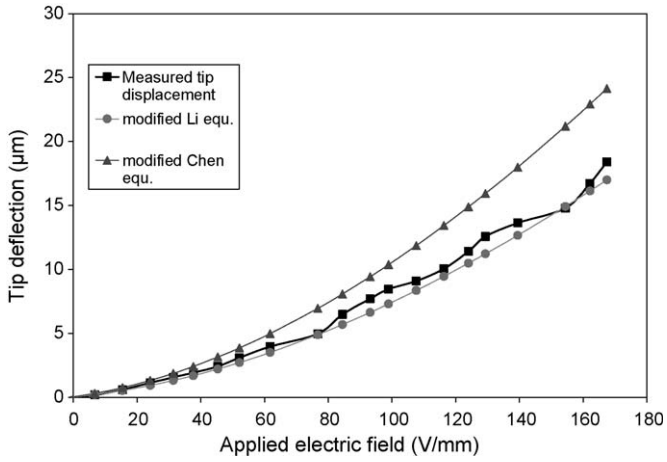

Fig. 10. Estimated and measured tip deflections of Tube A.

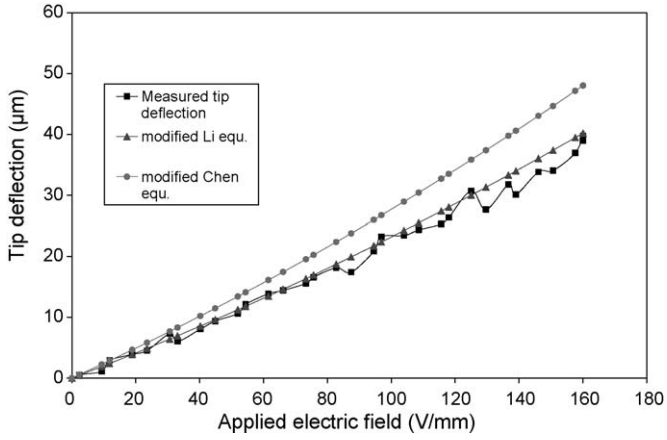

Fig. 11. Estimated and measured tip deflections of Tube B.

compared with the measured values. Li's modified equation, on the other hand, produces on average a deviation of 9% and hence is shown to model tubes of type A more appropriately.

Tube B has a thinner wall than Tube A with a 'wall thickness to radius' ratio of 0.30. The deflection of Tube B, as shown in Fig. 11, indicates that the modified Li equation is a good estimator of the actual deflection of the tube with a deviation of

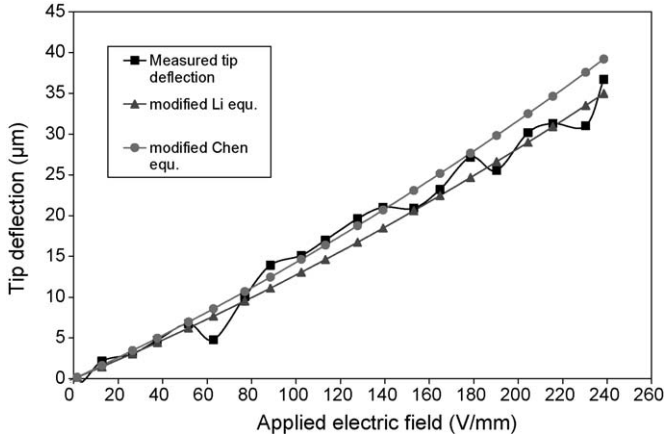

Fig. 12. Estimated and measured tip deflections of Tube C.

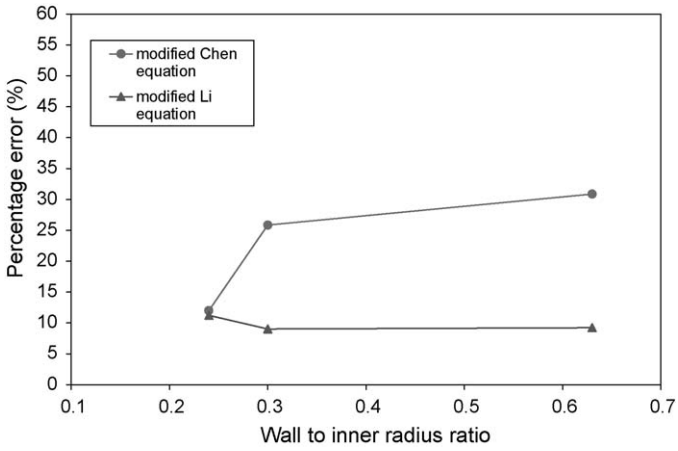

Fig. 13. Error in percentage of modified Li and Chen equations in comparison with the measured data.

9% on average. The modified Chen equation is less suitable resulting in a deviation on average of 26%.

Tube C is the thinnest tube produced with a 'wall thickness to radius' ratio of 0.23. As shown in Fig. 12, the theoretical estimates from the modified Chen and Li modified tip deflection equations and the measured values are close, with deviations of 12% and 11%, respectively. These results show that both equations predict reasonably well the tip deflections of thin-walled tubes.

6. Conclusions

The modified Chen equation gives a significant deviation for thick-walled tubes as shown in Fig. 13. When the tubes become thinner, Chen's modified equation can more closely predict the real tip deflections. With a 'wall thickness to radius' ratio of 0.23, the predicted and measured values become similar for both modified equations. It can be concluded that the modified Li equation gives good estimates of tip deflection of piezoelectric tubes with varying wall thicknesses. The modified Chen equation, which is computationally simpler and easier to use than the Li equation, gives good estimation with less than 15% deviation only for thin-walled tubes with a 'wall thickness to radius' ratio of less than 0.25.

Acknowledgments

This work was supported by a New Zealand FRST/NERF project. The authors would like to express their appreciation to Prof. Ma Jan and Dr Li Tao from Nanyang Technological University in Singapore for their assistance on piezoelectric tube development.

References

[1] C.J. Chen, Electromechanical deflections of piezoelectric tubes with quartered electrodes, Applied Physics Letters 60 (1) (1991) 132–134.
[2] T. Li, J. Ma, A piezoelectric tube with a double-layer configuration, Ceramics International 30 (7) (2004) 1803–1805.

[3] E. Haemmerle, M. Leung, K.A. Razak, M. Hodgson, W. Gao, Piezoceramic switches for optical fibres, Key Engineering Materials 352 (2007) 271–276.
[4] M. Leung, J. Yue, K.A. Razak, E. Haemmerle, M. Hodgson, W. Gao, Development of a 1 × 2 piezoelectric optical fiber switch, in: Proceedings of SPIE MEMS/MOEMS Technologies and Applications, vol. 6836, 2007.
[5] J. Yue, M. Leung, E. Haemmerle, M. Hodgson, G. Li, W. Gao, The influence of sintering conditions on the dielectric and piezoelectric properties of PbZrTiO–PbMgNbO ceramic tubes, Journal of Alloys and Compounds, doi:10.1016/j.jallcom.2008.02.107.
[6] N.R. Bauld, Mechanics of Materials, Wadsworth, California, 1982.
[7] T. Tsurumi, Non-linear piezoelectric and dielectric behaviours in perovskite ferroelectrics, Journal of the Ceramic Society of Japan 115 (1) (2007) 17–22.